



ORIGINAL ARTICLE

Valorization of two waste streams into activated carbon and studying its adsorption kinetics, equilibrium isotherms and thermodynamics for methylene blue removal



Zeid Abdullah AlOthman ^a, Mohamed Abdelaty Habila ^{a,*}, Rahmat Ali ^a,
Ayman Abdel Ghafar ^a, Mohamed Salah El-din Hassouna ^b

^a Department of Chemistry, College of Science, King Saud University, P.O. Box 2455, Riyadh 11451, Saudi Arabia

^b Department of Environmental Studies, Institute of Graduate Studies and Research, Alexandria University, 163 El-Horreya Avenue, P.O. Box 832, Alexandria, Egypt

Received 13 October 2012; accepted 14 May 2013

Available online 22 May 2013

KEYWORDS

Copyrolysis;
Agricultural waste;
Lubricating oil waste;
Activated carbon;
Adsorption;
Kinetic models

Abstract Wastes must be managed properly to avoid negative impacts that may result. Open burning of waste causes air pollution which is particularly hazardous. Flies, mosquitoes and rats are major problems in poorly managed surroundings. Uncollected wastes often cause unsanitary conditions and hinder the efforts to keep streets and open spaces in a clean and attractive condition. During final disposal methane is generated, it is much more effective than carbon dioxide as a greenhouse gas, leading to climate change. Therefore, this study describes the possible valorization of two waste streams into activated carbon (AC) with added value due to copyrolysis. High efficiency activated carbon was prepared by the copyrolysis of palm stem waste and lubricating oil waste. The effects of the lubricating oil waste to palm stem ratio and the carbonization temperature on the yield and adsorption capacity of the activated carbon were investigated. The results indicated that the carbon yield depended strongly on both the carbonization temperature and the lubricating oil to palm stem ratio. The efficiency of the adsorption of methylene blue (MB) onto the prepared carbons increased when the lubricating oil to palm stem ratio increased due to synergistic effect. The effects of pH, contact time, and the initial adsorbate concentration on the adsorption of methylene blue were investigated. The maximum adsorption capacity (128.89 mg/g) of MB occurred at pH 8.0.

* Corresponding author. Address: Department of Chemistry, College of Science, Building # 5, P.O. Box 2455, King Saud University, Riyadh 11451, Saudi Arabia. Tel.: +966 595184785.

E-mail address: mhabila@ksu.edu.sa (M.A. Habila).

Peer review under responsibility of King Saud University.



Production and hosting by Elsevier

The MB adsorption kinetics were analyzed using pseudo-first order, pseudo-second order and intraparticle diffusion kinetic models. The results indicated that the adsorption of MB onto activated carbon is best described using a second order kinetic model. Adsorption data are well fitted with Langmuir and Freundlich isotherms. The thermodynamic parameters; ΔG° , ΔH° and ΔS° indicate that the adsorption is spontaneous and endothermic.

© 2013 Production and hosting by Elsevier B.V. on behalf of King Saud University.

1. Introduction

Agricultural wastes are produced from farming activities, including planting and marketing; therefore various residues, by-products and remains are generated. Plant stems and corn-cobs are the most abundant components of solid agricultural waste (Tchobanoglous and Kreith, 2002). Each year, date palm trees must be pruned to remove old, dead or broken leaves. In the Kingdom of Saudi Arabia, this practice produces each year approximately 100,000 tons of date palm waste (Al-Jurf, 1988). Also used lubricating oil is produced in very large amount in Kingdom of Saudi Arabia due to large number of cars and long distance travel. These large amounts of waste can be converted into activated carbon, which is perhaps the most widely used adsorbent material for removing organic and inorganic pollutants from water and wastewater. The process for producing high-efficiency activated carbon is not completely investigated in developing countries. Furthermore, there are many problems with the regeneration of used activated carbon. Nowadays, there is a great interest in finding inexpensive and effective alternatives to the existing commercial activated carbon (Soylak and Dogan, 1996; Soyлак et al., 1999; Lili et al., 2009; Ghaedi et al., 2011, 2012). Exploring effective and low-cost activated carbon may contribute to environmental sustainability and offer benefits for future commercial applications. The costs of activated carbon prepared from biomaterials are very low compared to the cost of commercial activated carbon. Waste materials that have been successfully used to manufacture activated carbon in the recent past include waste apricots (Onal et al., 2007), rubber seed coat (Rengaraj et al., 2002), plum kernels (Tseng, 2007), apricot shell (Karagozoglu et al., 2007), rice straw (Daifullah et al., 2007; Wang et al., 2007), bamboo (Hameed et al., 2007), sunflower seed hull (Thinakaran et al., 2008), agricultural waste (Singh et al., 2008), mixed solid waste (AlOthman et al., 2011b) and rubber wood sawdust (Kumar et al., 2006).

The preparation of activated carbon in laboratory-scale can be categorized into two groups: synchronous carbonization and activation (i.e., a one-stage process), and an asynchronous process in which a separate carbonization process is performed before the activation process (i.e., a two-stage process) (Minkova et al., 1991). If the raw material is heat-treated by one of the above-mentioned processes, the resultant activated carbons should have different burn-off ratios and, thus, different pore characteristics and adsorption capacities because of their distinctly different thermal histories. This process produces activated carbon with a high adsorption capacity (Sabio et al., 1996). Pyrolysis is a good method for waste treatment and at the same time produces high efficiency activated carbon. Many authors have studied the pyrolysis of biomass and plastic waste and have demonstrated that it is a suitable waste processing (Scott and Czernic, 1990; Conesa et al., 1997; Kaminsky

et al., 1997; Williams and Williams, 1997; Lee and Shin, 2007). In the recent years, a novel approach to the wastes' recovery via their co-processing has been proposed. The existence of synergistic effects between the blend components during their conversion into solid products is still an open issue. Some authors have observed the absence of synergistic effects (Pinto et al., 2003), whereas evidence of their presence has been reported for co-gasification (Chmielniak and Sciazko, 2003) and co-pyrolysis (Collot et al., 1999).

Methylene blue is a dark-green powder or a crystalline solid cationic dye (Han et al., 2006). This dye is usually selected as a model compound for evaluating the adsorption efficiency of activated carbon (El Qada et al., 2006). In addition, MB is useful as an indicator for evaluating the adsorption capacity of activated carbon in liquid-phase adsorption (Tor and Cengeloglu, 2006). Also MB is usually discharged in high levels in industrial wastewater, specially textiles, paper and cosmetics industries. The complex structure of MB dye makes it very stable and difficult to degrade leading to many environmental problems such as preventing sunlight penetration into water, reducing photosynthetic activity and causing bad appearance of water surfaces (Dursun et al., 2007; Chih et al., 2009). Thus, the goals of this study were to enhance the efficiency of waste activated carbon in MB removal. The copyrolysis of palm stems and lubricating oil waste as well as chemical activation with K_2SO_4 was used to enhance the efficiency of waste activated carbon. The effect of the carbonization temperature and mixing ratio (lubricating oil to palm waste) on the properties of the activated carbon was investigated. The adsorptive properties of the prepared activated carbon were also evaluated using a model compound, MB. The effects of pH, contact time, and the initial adsorbate concentration on the adsorption of methylene blue were investigated. The MB adsorption kinetics were analyzed using pseudo-first order, pseudo-second order and intraparticle diffusion kinetic models.

2. Materials and methods

2.1. Materials

The precursors used in this study included the stems of palm trees collected from the agricultural solid waste in Riyadh, Saudi Arabia. Lubricating oil waste was collected from a petrol station in Riyadh. The palm waste was washed with distilled water to remove sand and dirt and then soaked in a 10% acid solution to remove fiber and traces of inorganic residue. The wastes were then dried in an oven at 110 °C for 24 h and crushed and ground into 0.5–2.0 mm particle size. The proximate and ultimate analyses of the palm wastes and lubricating oil were determined according to ASTM standard techniques, and the results are provided in Table 1.

Table 1 Ultimate and proximate analysis of the precursor materials.

Proximate analysis (wt. %)	Ultimate analysis (wt. %)	
	Palm stem	Lubricating oil
Moisture	6.06	0.373
Volatile matter	72.39	62
Ash	4.02	1.09
Fixed carbon	17.53	36.53

Ultimate analysis (wt. %)	Proximate analysis (wt. %)	
	Palm stem	Lubricating oil
Carbon	45.56	84.66
Hydrogen	5.91	13.51
Nitrogen	0.82	0
Oxygen	47.71	0

2.2. Activated carbon preparation

In this study, the three-stage process, which was reported by [Reinoso and Sabio \(1992\)](#), was used to prepare the activated carbon from the mixed wastes. In this process, the precursors are carbonized, impregnated, and then activated for a specific length of time. The lubricating oil and the ground palm stems were mixed in different weight ratios (0, 0.33, 0.5, and 1), placed into a 28 × 3.0 cm stainless steel vessel with an airtight lid, and carbonized in a muffle furnace under a self-generated atmosphere. The carbonization was conducted at two different temperatures (300 and 400 °C) for 2 h. The char produced was impregnated with K₂SO₄ by mixing 30 g of char with 10 g of K₂SO₄ in 50 mL of deionized water. The slurry was kept in an ultrasonic bath at 40 °C for 1 h to allow the maximum penetration of the solute molecules into the texture of the materials. The homogenous slurry was dried at 110 °C for 20 h, and the resulting impregnated char was activated at 450 °C for 1 h in a muffle furnace under a self-generated atmosphere. The obtained activated carbon was allowed to cool and washed with a 0.2 M HCl solution for 30 min to remove surface ash. The samples were washed repeatedly with distilled water until the pH of the filtrate reached approximately 6–7. After washing, the samples were dried at 110 °C for 24 h and allowed to cool in a desiccator. The samples were then filtered through a 100 μm mesh (US Standard) filter, retained on a 300 μm mesh filter, and stored in airtight bottles for further study. The carbon yield of each sample was calculated using Eq. (1).

$$\text{Yield}(\%) = W_1/W_o \times 100 \quad (1)$$

where W_1 is the dry weight (g) of the final activated carbon and W_o is the dry weight (g) of the precursor material.

2.3. Characterization of the activated carbon

2.3.1. Physical and elemental analyses

The pH of the prepared activated carbon samples was measured using a Metrohm model 744 pH meter (Switzerland). The bulk or apparent density was determined using a standard procedure where a known volume of the gently tapped activated carbon was weighed in a graduated cylinder. The apparent density was calculated as the ratio between the weight and the known volume of the closely packed sample. The elemental analysis was performed using a CHNS/O analyzer (Perkin Elmer PE2400 series II, USA).

2.3.2. Scanning electron microscopy

The surface morphology of the activated carbon particles was analyzed using a scanning electron microscope (JEOL-JSM-6380 LA, Japan). The carbon particles were mounted on sample stubs and coated with gold foil using a gold-coating

machine (JEOL-JSM-420, Japan). The samples were then automatically analyzed using computer software.

2.3.3. Methylene blue adsorption capacity

The adsorption capacity of the activated carbons was evaluated using MB as an adsorbate. A batch method was used to examine the MB adsorption capacity of the prepared activated carbons. First, 80 mL of the 50 mg/L MB solutions was mixed with 0.03 g of each sample and shaken for 24 h at 30 °C and 200 rpm. After this period, the residual concentration was determined spectrophotometrically at the corresponding $\lambda_{\text{max}} = 665$.

2.3.4. Batch adsorption studies

Mixed waste activated carbon was used for the adsorption studies. Activated carbon obtained from the coprolysis of palm stems and lubricating oil in a 1:1 ratio at a carbonization temperature of 400 °C followed by activation with K₂SO₄ was used for all of the adsorption studies.

The adsorption capacity of the activated carbon was evaluated using MB as an adsorbate. The adsorption was determined using a batch method, which allows for the convenient evaluation of parameters that influence the adsorption process. A stock solution of MB (1000 mg/L) was prepared in double-distilled water and further diluted to the desired concentrations. The batch adsorption experiments were performed in 250 mL conical flasks by mixing 80 mL of the MB solution with 0.03 g of activated carbon and then equilibrated in a thermostat-cum-shaking assembly (model MSW 275) at 30 °C and 200 rpm. After equilibrating, the concentration of remaining MB in the solution was measured using a UV-visible spectrophotometer (UV-30 LC, Thermo Scientific, England) at $\lambda_{\text{max}} = 665$. The amount of MB per unit weight of adsorbent, q_e (mg/g), was calculated using the following equation:

$$q_e = \frac{V(C_o - C_e)}{W} \quad (2)$$

where C_o and C_e are the initial and equilibrium concentrations of MB in solution (mg/L), V is the solution volume (L), W is the weight of the adsorbent (g) and q_e is the adsorption capacity (mg/g).

The effect of the initial pH on the removal of MB was examined over the pH range of 2–12 using 80 mL solutions with a MB concentration of 50 mg/L. The solution pH was adjusted to the desired value by the addition of 0.1 M HCl or NaOH.

The effect of shaking time on the adsorption of MB was examined at three different initial concentrations (30, 50, 100 mg/L) of MB at 30 °C, 0.03 g of adsorbent and the selected pH. At predetermined times; the solution of the specified flask was filtered using Whatman no. 42 filter paper and analyzed using a UV-visible spectrophotometer.

Table 2 Yield (wt. %), pH and density of carbon samples obtained from the co-pyrolysis of palm stems and lubricating oil at different temperatures.

Temp (°C)	Lubricating oil: palm stem ratio	Yield (%)	pH	Bulk density (g/cm ³)
300	0.0:1.0	37.06	3.51	0.60
	0.33:1.0	37.69	4.35	0.58
	0.5:1.0	38.27	3.71	0.56
	1.0:1.0	39.40	3.93	0.55
400	0.0:1.0	29.12	3.37	0.58
	0.33:1.0	29.73	3.88	0.56
	0.5:1.0	30.30	3.56	0.55
	1.0:1.0	31.53	3.42	0.53

3. Results and discussion

3.1. Yield and physical properties of the prepared activated carbon

The overall yields of the activated carbon samples obtained at different carbonization temperatures using different ratios of palm stems to lubricating oil are listed in Table 2. It is clear from Table 2 that the yield was significantly dependent on both the carbonization temperature and the palm stem to lubricating oil ratio. The yield increased as the lubricating oil to palm stem ratio increased from 0 to 1 and decreased when the carbonization temperature increased from 300 to 400 °C. The increase in carbonization temperature accelerated the dehydration and elimination reactions, resulting in an increase in the evolution of volatile matter and a decrease in the carbon yield. The decrease in the bulk density by increasing the carbonization temperature or the palm stem to lubricating oil ratio indicates the porosity of the prepared material.

3.2. Ultimate and proximate composition

ASTM techniques were used to determine the proximate and ultimate composition of the precursor materials and prepared activated carbon samples, and the results are shown in Table 3. Table 3 clearly shows that the volatile matter and moisture content of the activated carbons obtained from the copyrolysis of palm stems and lubricating oil at different carbonization temperatures decreased when the lubricating oil to palm stem ratio increased from 0 to 1, whereas the ash content increased. Temperature had the same effect; increasing the temperature from 300 to 400 °C promoted excessive burn-off, thereby lowering the yield and increasing the ash content. Data from the ultimate analyses of the prepared activated carbon samples are presented in Table 3. Using lubricating oil during pyrolysis increased the carbon content (fixed carbon and elemental carbon). The elemental carbon content was consistent with that of fixed carbon, with the fixed carbon content being lower than that of elemental carbon for each sample.

3.3. SEM images

Scanning electron micrographs (SEM) of the prepared carbon samples are shown in Figs. 1 and 2. The SEM images clearly indicate that the external surfaces of the samples were rough

and contained pores of various sizes and shapes. The surface had narrow elongated pores, which are consistent with the well-developed porosity. The micrographs revealed that the cavities on the surfaces of the carbon samples resulted from the evaporation of the K₂SO₄ during activation at moderate temperatures, creating an empty space. During impregnation, the molecules of the chemical impregnating agent diffused into the texture of the lignocellulosic material. During heat treatment at the desired temperature, the chemical impregnating agent evaporated and created the remaining porous carbon texture (Kütahyalı and Eral, 2004).

3.4. Methylene blue adsorption capacity

The adsorption capacity of the prepared activated carbon samples was examined by the MB uptake. Fig. 3(a) and (b) shows that the adsorption of MB increased when the lubricating oil to palm stem ratio increased from 0 to 1. The activated carbon obtained from palm stems without lubricating oil had a low adsorption capacity compared to those obtained from the copyrolysis of palm stems and lubricating oil. The lubricating oil increased the carbon content (fixed and elemental carbon) of the carbon samples, which resulted in highly porous carbon upon chemical activation. The porosity of the carbon samples obtained at different ratios of lubricating oil to palm stems (0.0, 0.33, 0.5 and 1) is also evident in the scanning electron microscope images (Figs. 1 and 2). Greater carbon porosity makes the carbon more accessible to the bulky molecules of MB, thereby increasing the MB removal efficiency. The carbonization temperature also had a considerable effect on the adsorption capacity of the prepared activated carbons. The adsorption capacity of the carbon samples increased when the carbonization temperature increased from 300 to 400 °C; increasing the carbonization temperature widens the pores, thereby improving MB's access. The adsorption capacity of MB for carbon produced at 400 °C, for 2 h and activated with K₂SO₄ was the highest. Efficiency of commercial activated carbon is added for comparison. Efficiency of the prepared activated carbon is in competition with commercial activated carbon.

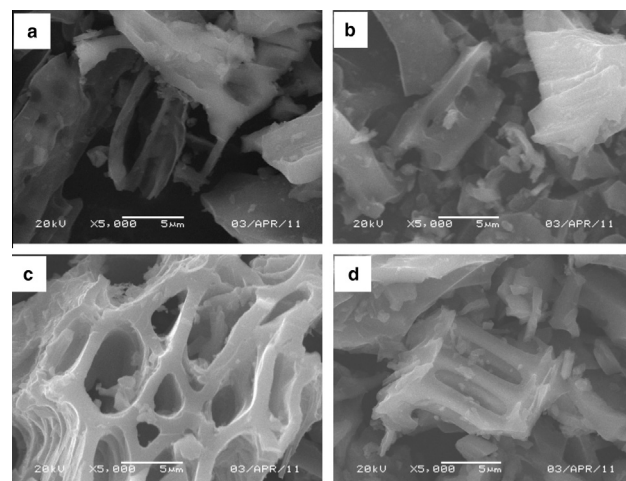
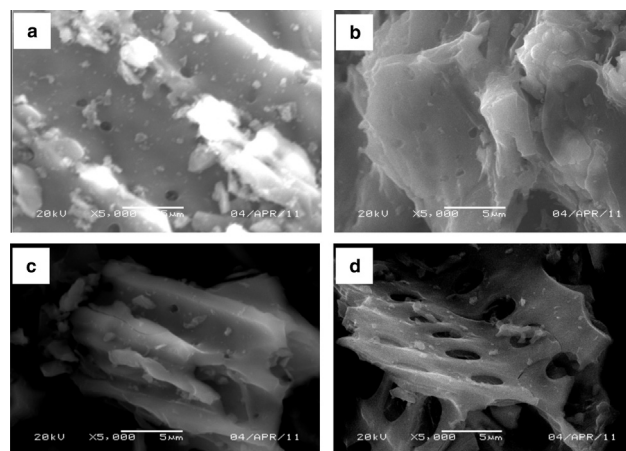
3.5. Batch adsorption studies

3.5.1. Effect of pH

The pH of aqueous solution is one of the most important factors in the adsorption of cationic dyes because of its impact on both the surface binding-sites of the adsorbent and the ionization process of the dye molecule (Wang et al., 2008). MB is basic in nature; therefore, it releases colored dye cations into solution on dissolution. The adsorption of MB onto the surface of an adsorbent is primarily influenced by the surface charge of the adsorbent, which is in turn influenced by the solution pH. The effect of the initial solution pH on the adsorption of MB was examined over a pH range of 2–12 at an initial concentration of 50 mg/L, as shown in Fig. 4. It is clear from this figure that the adsorption capacity increased when the initial solution pH increased, but the percentage removal of MB only changes slightly above pH 8. After 24 h, the amount of MB adsorbed was 51.13 (mg/g) at pH = 2 and had increased to 92.06 (mg/g) at pH 8. This may be due to the formation of more negatively charged groups on the

Table 3 Proximate and ultimate analyses of the activated carbon prepared by the copolyolysis of palm stems and lubricating oil at different carbonization temperatures.

Temp. (°C)	Lubricating oil/palm stem ratio	Char/K ₂ SO ₄ ratio	Proximate analysis			Ultimate analysis				
			Moisture	Volatiles matter	Ash	Fixed carbon	C	H	N	O
300	0	0	2.10	33.49	3.79	60.62	72.13	2.58	0.79	24.50
	0.33	3:1	2.57	33.44	3.80	60.19	72.94	2.79	0.64	23.63
	0.5	3:1	2.19	28.44	4.15	65.22	73.93	2.88	0.79	22.40
	1	3:1	1.59	25.82	4.67	67.92	74.84	2.75	0.48	21.93
400	0	0	2.44	30.19	5.34	62.03	73.69	2.39	0.89	23.03
	0.33	3:1	2.39	30.62	4.61	62.38	74.07	2.41	1.06	22.46
	0.5	3:1	1.99	26.94	4.97	66.10	74.22	2.42	0.73	22.63
	1	3:1	1.37	24.66	5.29	68.68	74.84	2.20	0.90	22.06

**Figure 1** Scanning electron microscope images of activated carbon prepared by the copolyolysis of different ratios of lubricating oil and palm stems: (a) 0.0, (b) 0.33, (c) 0.5 and (d) 1.0 at 300 °C.**Figure 2** Scanning electron microscope images of activated carbon prepared by the copolyolysis of different ratios of lubricating-oil and palm stems, (a) 0.0, (b) 0.33, (c) 0.5 and (d) 1.0, at 400 °C.

surface of the adsorbent, which is necessary for the adsorption of a basic dye. At pH 2.0, there is a net positive charge because of the presence of H⁺; the competition of H⁺ with the dye cations resulted in the active sites becoming protonated and thus unavailable to the dye cations. However, at higher pH values, more negatively charged surface sites are available, which facilitates the adsorption of dye cations.

3.5.2. The effects of contact time and initial concentration

The amount of MB adsorbed onto the activated carbon was examined as a function of the shaking time at different initial concentrations at 30 °C and the chosen pH. The effect of contact time on the adsorption of MB, at three different concentrations (30, 50, 100 mg/L), of MB adsorption by activated carbon is shown in Fig. 5. It is evident from this figure that the amount of MB adsorbed increased with increasing contact

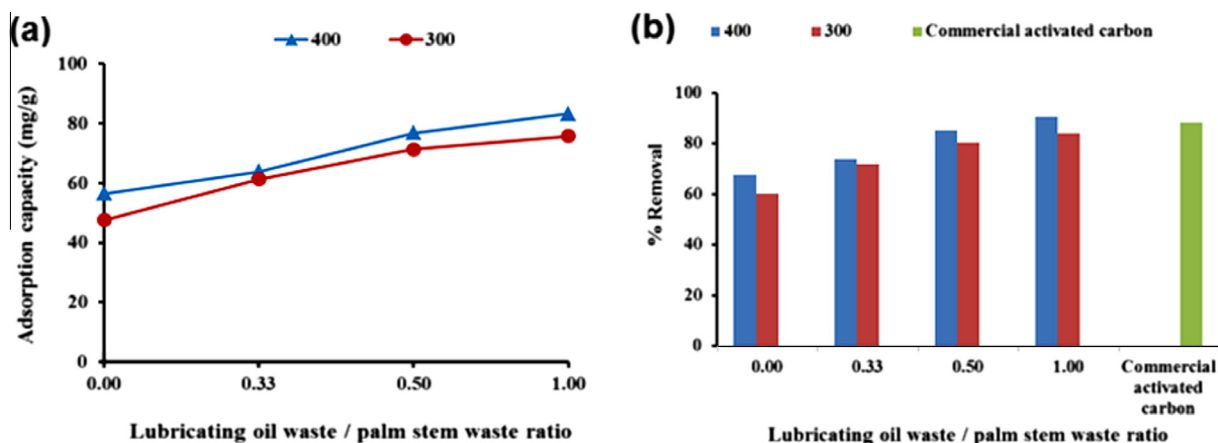


Figure 3 MB adsorption capacity (a) and adsorption efficiency (b) onto activated carbons prepared from the copyrolysis of lubricating oil and palm stems at different ratios (0.0, 0.33, 0.5 and 1.0) and carbonization temperatures. Experimental conditions: pH 8.0; 30 °C; adsorbent weight, 0.03 g.

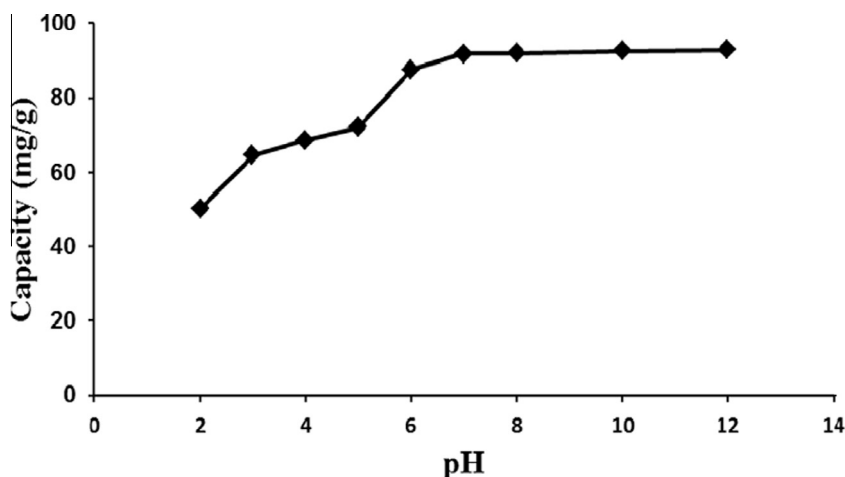


Figure 4 Effect of pH on the adsorption of MB at an initial feed concentration of 50 mg/L. Experimental conditions: 30 °C; adsorbent weight, 0.03 g.

time. Furthermore, the adsorption was rapid during the first 180 min and then gradually decreased to become constant after the equilibrium point. The rapid adsorption of MB cations during the initial stages may result from the availability of the uncovered surface and active sites on the adsorbent surface. The saturation point is almost reached at 480 min. The amount of dye adsorbed at the equilibrium time reflects the maximum adsorption capacity of the adsorbent. The removal of MB was dependent on the initial concentration. The amount of MB adsorbed, q_e (mg/g), increased with an increase in the initial concentration. In this study, the amount of MB adsorbed at equilibrium increased from 76 to 128.89 mg/g when the initial dye concentration increased from 30 to 100 mg/L. The mass transfer driving force increases when the initial concentration increased, thereby resulting in a higher adsorption of MB. At low concentrations, the ratio of the available surface area to the initial MB concentration is higher; therefore, the removal becomes independent of the initial concentration. However, in the case of higher concentrations, this ratio is low and, thus, the percentage removal depends upon the initial concentration.

3.5.3. MB adsorption kinetics

To examine the adsorption mechanism, the pseudo first-order (Singh and Tiwari, 1997), pseudo second-order (HO et al., 2000) and intraparticle diffusion (Srivastava et al., 1989) models were applied to analyze the experimental data from the adsorption of MB to the prepared activated carbon. The conformity between the experimental data and the values predicted by the models is expressed as correlation coefficients (R^2).

3.5.3.1. Pseudo-first-order kinetic model. The integral form of the Lagergren pseudo-first-order model is generally expressed as:

$$\log(q_e - qt) = \log q_e - \frac{k_1 t}{2.303} \tag{3}$$

where q_e and qt are the amounts of MB adsorbed (mg/g) at equilibrium and time t , respectively, and k_1 is the rate constant of the first-order adsorption (min^{-1}). Straight lines were obtained by plotting $\log(q_e - qt)$ against t , as shown in Fig. 6. The values of the rate constant, k_1 , and q_e at three different

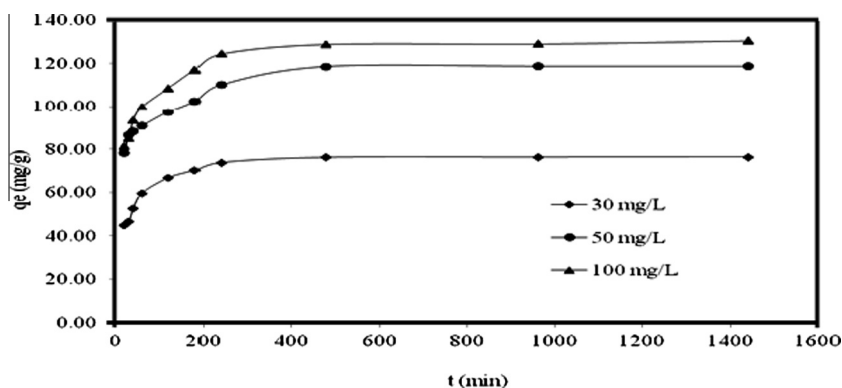


Figure 5 Effect of contact time on the MB adsorption to activated carbon at different concentrations. Experimental conditions: pH 8.0; 30 °C; adsorbent weight, 0.03 g.

initial methylene blue concentrations were obtained from the slopes and intercepts of the plots, respectively, and are presented in Table 4.

3.5.3.2. Pseudo-second-order kinetic model. The integrated form of the pseudo-second-order adsorption kinetic model is expressed as

$$\frac{t}{q_t} = \frac{1}{k_2 q_e^2} + \frac{t}{q_e} \quad (4)$$

where q_e and q_t are the sorption capacities (mg/g) at equilibrium and time t , respectively, and k_2 is the rate constant of the pseudo-second order sorption (g/mg.min).

The initial adsorption rate, h (mg/g.min), is given as

$$h = k_2 q_e^2 \quad (5)$$

The plots of t/q_t versus t of Eq. (4) are linear, as shown in Fig. 7. The values of q_e and k_2 were determined from the slopes and intercepts of the plots, respectively, and are listed in Table 4.

3.5.3.3. The intraparticle diffusion model. The intraparticle diffusion model was examined to identify the diffusion mechanism as follows:

$$qt = k_{id} t^{1/2} + C \quad (6)$$

where k_{id} is the intraparticle diffusion rate constant (mg/g min^{1/2}), and C is the intercept (mg/g).

The plots of qt versus $t^{1/2}$ were straight lines, as shown in Fig. 8. The values of k_{id} were calculated from the slopes of the plots. The C values provided general information about the thickness of the boundary layer, i.e., the larger the intercept, the greater the contribution of the surface sorption in the rate-controlling step. The data for the adsorption of MB to the activated carbon used in the intraparticle diffusion model are shown in eight, and the results are given in Table 4.

The parameters of the pseudo-first order, pseudo-second order and intraparticle diffusion models are shown in Table 4. The results indicated that among these three models, the pseudo-second order kinetic equations had higher R^2 values and experimental q_e values that agree well with the calculated values. The low R^2 values for the pseudo-first order and intraparticle diffusion models indicated that these models did not fit the data well. Furthermore, for the pseudo-first order kinetic model, the experimental q_e was not in good agreement with the calculated q_e . Therefore, the pseudo-second order kinetic model provided the best description of the MB adsorption mechanism.

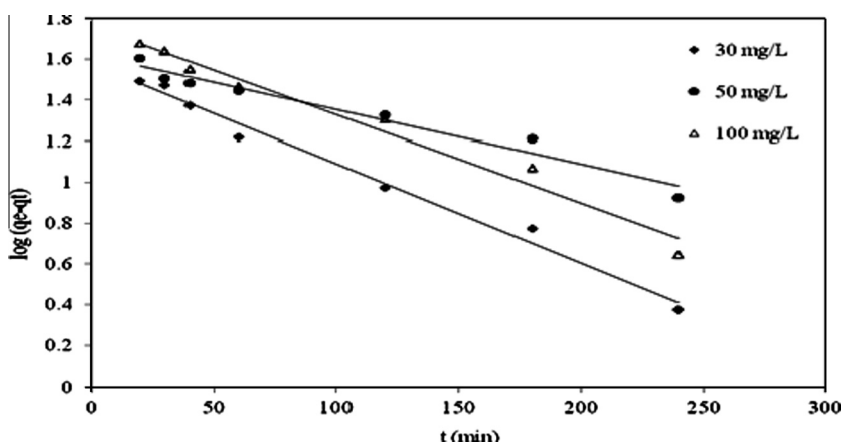


Figure 6 Lagergren first-order plot for the adsorption of MB to activated carbon at different concentrations. Experimental conditions: pH 8.0; 30 °C; adsorbent weight, 0.03 g.

Table 4 Kinetic constants obtained for the adsorption of MB onto activated carbon prepared from the copypolysis of lubricating oil and palm stems.

Pseudo-first order				Pseudo-second order				Intraparticle diffusion			
C_0 (mg/L)	q_e, exp (mg/g)	K_1 (10^{-3}) (min^{-1})	q_e, cal (mg/g)	R^2	k_2 (10^{-4}) (g/mg.min)	q_e, cal (mg/g)	h (mg/g.min)	R^2	k_{id} (mg/g.min)	C (mg/g)	R^2
30	76.09	1.300	37.731	0.897	6.605	78.740	4.095	0.999	2.654	34.917	0.947
50	118.67	9.903	57.809	0.959	7.473	112.359	9.434	0.996	2.483	70.775	0.962
100	128.89	14.44	41.639	0.974	4.650	129.870	7.843	0.997	3.781	66.906	0.979

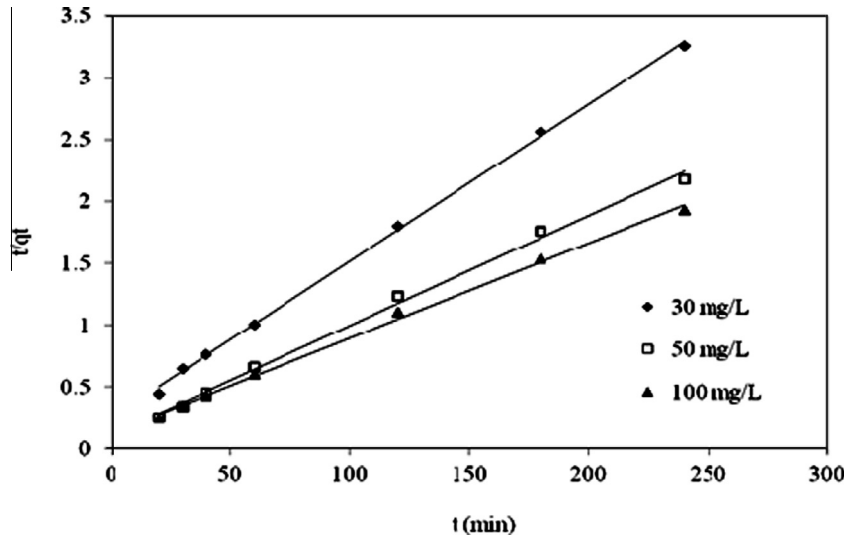


Figure 7 Pseudo-second order kinetic plot for the adsorption of MB by activated carbon at different concentrations. Experimental conditions: pH 8.0; 30 °C; adsorbent weight, 0.03 g.

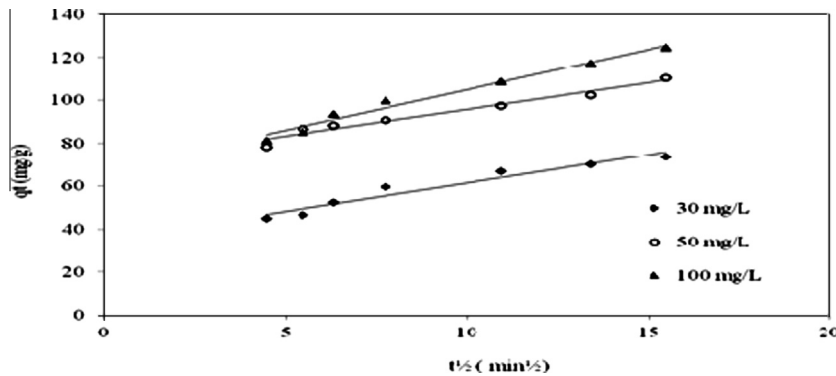


Figure 8 Intraparticle diffusion kinetic plot for the adsorption of MB by activated carbon at different concentrations. Experimental conditions: pH 8.0; 30 °C; adsorbent weight, 0.03 g.

3.5.4. Adsorption isotherms

The adsorption isotherm indicates how adsorbate molecules are distributed between the liquid and solid phases when the adsorption process is in an equilibrium state. Analysis of the isotherm data by fitting different isotherm models is an important step in determining a suitable model for design purposes (Chang and Chang, 2001). Fig. 9 shows Langmuir (a) and Freundlich (b) adsorption isotherms for MB adsorption onto prepared activated carbon at 25 °C and pH 8.

3.5.4.1. Langmuir isotherm. The Langmuir equation (Tjeerdema and Miltz, 2005) was applied to the equilibrium adsorption data for MB dye onto prepared activated carbon. The Langmuir treatment is based on the assumptions that maximum adsorption corresponds to saturated monolayer coverage of adsorbate molecules onto the adsorbent surface, that the energy of adsorption is constant and that there is no transmigration of adsorbate to the plane surface.

$$C_e/q_e = 1/(q_{max}.b) + C_e/q_{max}, \tag{7}$$

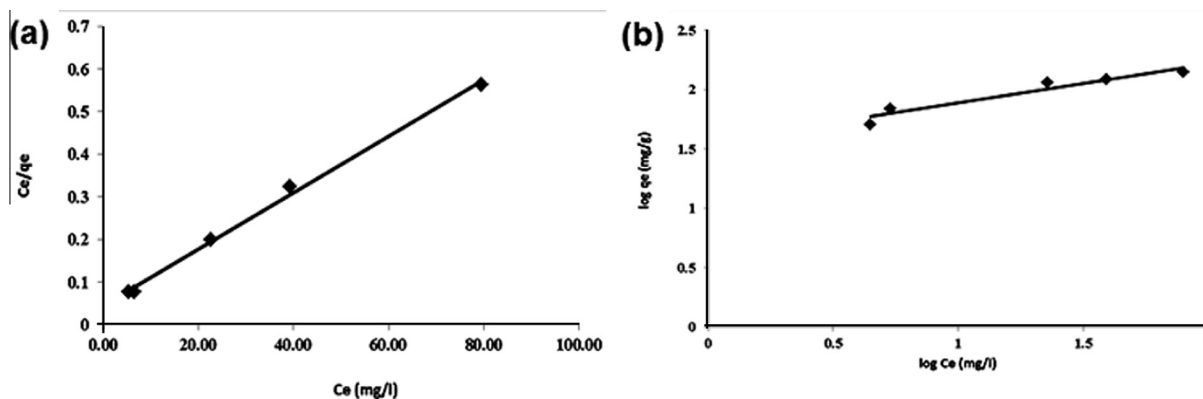


Figure 9 Langmuir (a) and Freundlich (b) isotherms for adsorption of MB dye onto prepared activated carbon.

Table 5 Langmuir and Freundlich constants for the adsorption of MB dye onto prepared activated carbon at pH 8 and 25 °C.

	Constant	Prepared activated carbon
Langmuir constants	K_L	966.4
	b	6.47
	Q_{max}	149.2
	R^2	0.99
Freundlich constants	K_F	36.15
	n	3.03
	R^2	0.927

where C_e is the equilibrium concentration of the adsorbate (mg/l), q_e is the amount of dye adsorbed (mg/g), and q_{max} and b are Langmuir constants related to the maximum adsorption capacity (mg/g) and the adsorption energy, respectively. The Langmuir equilibrium constant, K_L , can be obtained from:

$$K_L = q_{max} \cdot b \tag{8}$$

The linear form of the Langmuir isotherm is shown in Fig. 9. The correlation coefficients, R^2 , for the adsorption of MB dye onto prepared activated carbon are 0.96 and 0.976, respectively, indicating that the adsorption was well fitted by the Langmuir isotherm.

3.5.4.2. Freundlich isotherm. As shown in the following Eq. (9),

$$\text{Log}q_e = \text{log}K + 1/n\text{log}C_e, \tag{9}$$

where C_e is the equilibrium concentration (mg/l) and q_e is the amount of dye adsorbed (mg/g) at equilibrium. The quantities K_F and n are the Freundlich constants, with K_F (mg/g) indicating the adsorbent capacity and n indicating the favorable nature of the process. Plots of $\text{log } q_e$ versus $\text{log } C_e$ should be linear, with the slope and intercept of the line obtained corresponding to $1/n$ and $\text{log } K_F$, respectively (Fig. 9).

The calculated results of the Langmuir and Freundlich isotherm constants are given in Table 5. The adsorption of MB dye onto prepared activated carbon was well correlated with the Langmuir equation and Freundlich equation for the concentration range studied.

3.5.5. Thermodynamic studies

Thermodynamic parameters, such as change in Gibbs free energy (ΔG°), enthalpy (ΔH°) and entropy (ΔS°), were evaluated using Eqs. (10) and (11):

$$\text{Log}K_d = \Delta S^\circ / 2.303R - \Delta H^\circ / 2.303RT \tag{10}$$

$$\Delta G^\circ = -RT\text{ln}K_d \tag{11}$$

where K_d is the equilibrium partition constant calculated as the ratio between sorption capacity (q_e) and equilibrium concentration (C_e), R is the gas constant (8.314 J/mol/K) and T is the temperature in Kelvin (K). From Eq. (10) a plot of log

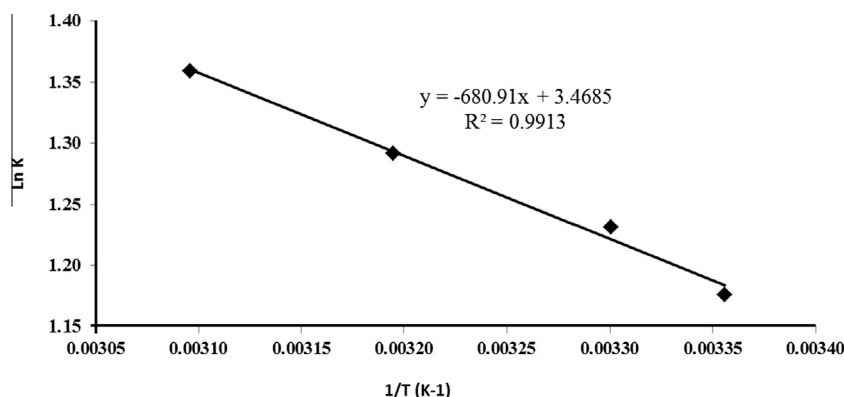


Figure 10 Thermodynamic study of adsorption of MB onto prepared activated carbon.

Table 6 Thermodynamic parameters of adsorption of MB onto prepared activated carbon.

Temperature $T(K)$	Thermodynamic parameters		
	ΔG° (kJ/mol)	ΔS° (J/mol/K)	ΔH° (kJ/mol)
298	-6.7	63.0	13.04
303	-7.1		
313	-7.7		
323	-8.4		

K_d vs. $1/T$ (Fig. 10) gives ΔH° and ΔS° , The calculated thermodynamic parameters are given in Table 6.

The negative value of ΔG° indicates the spontaneous nature of MB adsorption onto the prepared activated carbon. Generally, a value of ΔG° in between 0 and -20 kJ/mol is consistent with electrostatic interaction between adsorption sites and the adsorbing ion (physical adsorption) while a more negative ΔG° value ranging from -80 to -400 kJ/mol indicates that the adsorption involves charge sharing or transferring from the adsorbent surface to the adsorbing ion to form a coordinate bond (chemisorption) (Smith and Van Ness, 1987; Sigh, 2000; Horsfall et al., 2004; Malkoc and Nuhoglu, 2007; AlOthman et al., 2011a). As shown, the magnitude of ΔG° (-6.27 to -12 kJ/mol) indicates a typical physical process. According to the Van't Hoff equation, the standard enthalpy and the entropy values in the range of 25 – 50 °C were obtained as 44.13 kJ mol $^{-1}$ and 158.3 kJ mol $^{-1}$ K $^{-1}$ at initial pH 5 and initial MB concentration 50 ppm, respectively. As can be deduced from Fig. 10, the positive value of ΔH° suggests the endothermic nature of adsorption while the positive values of ΔS° indicate an increase in the degree of freedom (or disorder) of the adsorbed species. In general, the thermodynamic parameters indicate that the adsorption is spontaneous and endothermic.

4. Conclusion

Activated carbon was prepared by the copyrolysis of palm stems and lubricating oil waste through chemical activation with K_2SO_4 at different temperatures. The yield increased as the lubricating oil to palm stem ratio increased from 0 to 1 and decreased when the carbonization temperature increased from 300 to 400 °C. The volatile matter and moisture content of the activated carbon decreased when the lubricating oil to palm stem ratio increased from 0 to 1, whereas the ash content increased. Temperature had the same effect as the waste ratio: increasing the temperature from 300 to 400 °C promoted excessive burn-off, thereby lowering the yield and increasing the ash content. The activated carbon obtained from the copyrolysis of palm stems and lubricating oil in the ratio of 1:1 had a high adsorption capacity. The kinetics of MB adsorption were followed pseudo-second-order rate expressions. The thermodynamic parameters indicate that the adsorption is spontaneous and endothermic. The adsorption of MB was dependent on its initial concentration. The amount of MB adsorbed at equilibrium increased from 76 to 128.89 mg/g when the initial dye concentration increased from 30 to 100 mg/L.

Acknowledgment

This work was supported by King Saud University, Deanship of Scientific Research, College of Science Research Center.

References

- Al Othman, Z.A., Hashem, A., Habila, M.A., 2011a. Kinetic, equilibrium and thermodynamic studies of cadmium (II) adsorption by modified agricultural wastes. *Molecules* 16, 10443–10456.
- AlOthman, Z.A., Habila, M.A., Ali, R., 2011b. Preparation of Activated Carbon Using the Copyrolysis of Agricultural and Municipal Solid Wastes at a Low Carbonization Temperature. International Conference on Biology, Environment and Chemistry (ICBEC), Dubai, UAE (pp. 28–30).
- Al-Jurf, R.S., 1988. Development of heat insulating materials using date palm leaves. *J. Therm. Insul.* 11, 158–164.
- Chang, S.T., Chang, H.T., 2001. Comparisons of the photostability of esterified wood. *Polym. Degrad. Stab.* 71 (2), 261–266.
- Chih, H.W., Yao, T.L., Tai, W.T., 2009. Removal of methylene blue from aqueous solution by adsorption onto pineapple leaf powder. *J. Hazard. Mater.* 170, 417–424.
- Chmielniak, T., Sciazko, M., 2003. Co-gasification of biomass and coal for methanol synthesis. *Appl. Energy* 74 (3–4), 393–403.
- Collot, G., Zhuo, Y., Dugwell, D.R., Kandiyoti, R., 1999. Copyrolysis and co-gasification of coal and biomass in bench-scale fixed-bed and fluidized bed reactors. *Fuel* 78 (6), 667–679.
- Conesa, J.A., Font, R., Marcilla, A., Caballero, J.A., 1997. Kinetic model for the continuous pyrolysis of two types of polyethylene in a fluidized bed reactor. *J. Anal. Appl. Pyrolysis* 40 (41), 419–431.
- Daifullah, A.A.M., Yakout, S.M., Elreedy, S.A., 2007. Adsorption of fluoride in aqueous solutions using $KMnO_4$ -modified activated carbon derived from steam pyrolysis of rice straw. *J. Hazard. Mater.* 147, 633–643.
- Dursun, O., Gulbeyi, D., Ahmet, O., 2007. Methylene blue adsorption from aqueous solution by dehydrated peanut hull. *J. Hazard. Mater.* 144, 171–179.
- El Qada, E.N., Allen, S.J., Walker, G.M., 2006. Adsorption of methylene blue onto activated carbon produced from activated bituminous coal: a study of equilibrium adsorption isotherm. *Chem. Eng. J.* 124, 103–110.
- Ghaedi, M., Shokrollahi, A., Tavallali, H., Shojaiepoor, F., Keshavarzi, B., Hossainian, H., Soylak, M., Purkait, M.K., 2011. Activated carbon and multiwalled carbon nanotubes an efficient adsorbents for kinetic and equilibrium study of removal of arsenazo and methyl red dyes from waste water. *Toxicol. Environ. Chem.* 93, 438–449.
- Ghaedi, M., Najibi, A., Hossainian, H., Shokrollahi, A., Soylak, M., 2012. Kinetic and equilibrium study of alizarin red s removal by activated carbon. *Toxicol. Environ. Chem.* 94, 40–48.
- Hameed, B.H., Din, A.T.M., Ahmad, A.L., 2007. Adsorption of methylene blue onto bamboo-based activated carbon: kinetics and equilibrium studies. *J. Hazard. Mater.* 141, 819–825.
- Han, R., Zou, W., Yu, W., Cheng, S., Wang, Y., Shi, J., 2006. Biosorption of methylene blue from aqueous solution by fallen phoenix tree's leaves. *J. Hazard. Mater.* 141, 156–162.
- Ho, Y.S., Mckay, G., Wase, D.A.J., Foster, C.F., 2000. Study of the sorption of divalent metal ions on to peat. *Adsorpt. Sci. Technol.* 18, 639–650.
- Horsfall, M., Spiff, A.I., Abia, A.A., 2004. Studies on the influence of mercaptoacetic acid (MAA) modification of cassava (*Manihot sculenta* cranz) waste Biomass on the adsorption of Cu^{2+} and Cd^{2+} from aqueous solution. *Bull. Korean Chem. Soc.* 25, 969–976.
- Kaminsky, W., Kim, B.J., Schlesselmann, 1997. Pyrolysis of a fraction of mixed plastic wastes depleted in PVC. *J. Anal. Appl. Pyrolysis* 40 (41), 365–372.
- Karagozoglu, B., Tasdemir, M., Demirbas, E., Kobya, M., 2007. The adsorption of basic dye (Astrazon Blue FGRL) from aqueous solutions onto sepiolite, fly ash and apricot shell activated carbon: kinetic and equilibrium studies. *J. Hazard. Mater.* 147, 297–306.

- Kumar, B.G.P., Shivakamy, K., Miranda, L.R., Velan, M., 2006. Preparation of steam activated carbon from rubberwood sawdust (*Hevea brasiliensis*) and its adsorption kinetics. *J. Hazard. Mater.* 136, 922–929.
- Kütahyalı, C., Eral, M., 2004. Selective Adsorption of Uranium from Aqueous Solutions Using Activated Carbon Prepared from Char-coal by Chemical Activation. *J. Sep Purif Technol* 40, 109–114.
- Lee, K.W., Shin, D.H., 2007. Characteristics of liquid product from the pyrolysis of waste plastic mixture at low and high temperatures: influence of lapse time of reaction. *Waste Manage. (Oxford)* 27, 168–176.
- Lili, L., Liping, G., Chunjing, G., 2009. Adsorption of Congo red from aqueous solutions onto Ca-bentonite. *J. Hazard. Mater.* 161, 126–131.
- Malkoc, E., Nuhoglu, Y., 2007. Determination of kinetic and equilibrium parameters of the batch adsorption Cr (IV) onto waste acorn of *Quercusithaburensis*. *Chem. Eng. Process.* 46, 1020–1029.
- Minkova, V., Razvigorova, M., Goranova, M., Ljutzkanov, L., Angelova, G., 1991. Effect of water vapour on the pyrolysis of solid fuels. II. Effect of water vapour during the pyrolysis of solid fuels on the formation of the porous structure of semicoke. *Fuel* 70, 713–719.
- Onal, Y., Akmil-Basar, C., Sarici-Ozdemir, C., 2007. Elucidation of the naproxen sodium adsorption onto activated carbon prepared from waste apricot: kinetic, equilibrium and thermodynamic characterization. *J. Hazard. Mater.* 148, 727–734.
- Pinto, F., Franco, C., André, R.N., Tavares, C., Dias, M., Gulyurtlu, I., Cabrita, I., 2003. Effect of experimental conditions on co-gasification of coal, biomass and plastics wastes with air/steam mixtures in a fluidized bed system. *Fuel* 82 (15–17), 1967–1976.
- Reinoso, F.R., Sabio, M.M., 1992. Activated carbons from lignocellulosic materials by chemical and/or physical activation: an overview. *Carbon* 30 (7), 1111–1118.
- Rengaraj, S., Moon, S.H., Sivabalan, R., Arabindoo, B., Murugesan, V., 2002. Removal of phenol from aqueous solution and resin manufacturing industry wastewater using an agricultural waste: rubber seed coat. *J. Hazard. Mater.* 89, 185–196.
- Sabio, M.M., Gonzalez, M.T., Reinoso, F.R., Escribano, A.S., 1996. Effect of steam and carbon dioxide activation in the micropore size distribution of activated carbon. *Carbon* 34 (4), 505–509.
- Scott, D.S., Czernic, S.R., 1990. Fast pyrolysis of plastic wastes. *Energy Fuels* 4, 407–411.
- Sigh, D., 2000. Studies of the adsorption thermodynamics of oxamyl on fly ash. *Adsorpt. Sci. Technol.* 18, 741–748.
- Singh, V.K., Tiwari, P.N., 1997. Removal and recovery of chromium (VI) from industrial waste water. *J. Chem. Technol. Biotechnol.* 69, 376–382.
- Singh, K.P., Malik, A., Sinha, S., Ojha, P., 2008. Liquid-phase adsorption of phenols using activated carbons derived from agricultural waste material. *J. Hazard. Mater.* 150, 626–641.
- Smith, J.M., Van Ness, H.C., 1987. *Introduction to Chemical Engineering Thermodynamics*, fourth ed. McGraw-Hill, Singapore.
- Soylak, M., Dogan, M., 1996. Column preconcentration of trace amounts of copper on activated carbon from natural water samples. *Anal. Lett.* 29, 635–643.
- Soylak, M., Narin, I., Elci, L., Dogan, M., 1999. Atomic absorption spectrometric determination of copper, cadmium, lead and nickel in urine samples after enrichment and separation procedure on an activated carbon column. *Trace Elem. Electrolytes* 16, 131–134.
- Srivastava, S.K., Tyagi, R., Pant, N., 1989. Adsorption of heavy metal ions on carbonaceous material developed from the waste slurry generated in local fertilizer plants. *Water Res.* 23, 1161–1165.
- Tchobanoglous, G., Kreith, F., 2002. *Handbook of Solid Waste Management*. McGraw-hill, New York.
- Thinakaran, N., Baskaralingam, P., Panneerselvam, M.P., Sivanesan, S., 2008. Removal of acid violet 17 from aqueous solutions by adsorption onto activated carbon prepared from sunflower seed hull. *J. Hazard. Mater.* 151, 316–322.
- Tjeerdsma, B.F., Militz, H., 2005. Chemical changes in hydrothermal treated wood: FTIR analysis of combined hydrothermal and dry heat-treated wood. *Eur. J. Wood Wood Prod.* 63 (2), 102–111.
- Tor, A., Cengeloglu, Y., 2006. Removal of Congo red from aqueous solution by adsorption onto acid activated red mud. *J. Hazard. Mater.* 138, 409–415.
- Tseng, R.L., 2007. Physical and chemical properties and adsorption type of activated carbon prepared from plum kernels by NaOH activation. *J. Hazard. Mater.* 147, 1020–1027.
- Wang, S.L., Tzou, Y.M., Lu, Y.H., Sheng, G., 2007. Removal of 3-chlorophenol from water using rice-straw-based carbon. *J. Hazard. Mater.* 147, 313–318.
- Wang, X.S., Zhou, Y., Yu, J., Sun, C., 2008. The removal of basic dyes from aqueous solutions using agricultural by-products. *J. Hazard. Mater.* 157, 374–385.
- Williams, E.A., Williams, P.T., 1997. Analysis of products derived from the fast pyrolysis of plastic waste. *J. Anal. Appl. Pyrolysis* 40 (41), 347–363.